SESSION 8

https://doi.org/10.1017/S1743921319008263 Published online by Cambridge University Press

Laboratory Astrophysics: from Observations to Interpretation
Proceedings IAU Symposium No. 350, 2019
F. Salama & H. Linnartz, eds.
doi:10.1017/S1743921319008263

Gas-dust chemistry of volatiles in the star and planetary system formation

Yuri Aikawa[1] and Kenji Furuya[2]

[1]Department of Astronomy, The University of Tokyo, 113-0033, Tokyo, Japan
email: aikawa@astron.s.u-tokyo.ac.jp

[2] Center for Computational Sciences, University of Tsukuba, 1-1-1 Tennodai, Tsukuba, Ibaraki 305-8577 Japan,
email: furuya@ccs.tsukuba.ac.jp

Abstract. The focus of this work is on two topics: (i) formation of complex organic molecules (COMs) and (ii) isotope fractionation. Various COMs, which are C, H-containing molecules consisting of 6 atoms and more, have been detected in the central warm region of protostellar cores. Most of this review is about gas-grain chemical models, which have been constructed to evaluate the mechanisms and efficiency of the COM formation. The relevant physical and chemical processes are investigated in laboratory experiments, as reported in other articles in this volume.

The isotope fractionation of volatile elements is observed in both the interstellar medium (ISM) and Solar system material. While exothermic exchange reactions enrich molecules with heavier isotopes such as Deuterium, the isotope selective photodissociation can be coupled with ice formation to enrich the ice mantle with rare isotopes. The efficiency of this fractionation depends on the photodesorption yields, which has been studied in laboratory experiments.

Keywords. interstellar matter, astrochemistry, star-formation

1. Introduction

How the ISM evolves and is incorporated to planetary system material is one of the most intriguing questions in the study of star- and planetary system formation. Thanks to the high sensitivity and spatial resolution of Atacama Large Millimeter and submillimeter Array (ALMA), it has become possible to directly observe the vicinity ($\leqslant 100$ au) of low-mass young stellar objects, where a protoplanetary disk emerges from the infalling ISM (Figure 1a). Due to the heating by protostellar irradiation and release of gravitational energy, various molecules are sublimated to the gas phase. Detected molecules include COMs, such as CH_3OH, CH_3CHO, and CH_3OCH_3. COMs are also detected in comets in our Solar system, indicating a possible link between the ISM and planetary system material. The isotope fractionation is another key to investigate the link. The high HDO/H_2O ratio ($\sim 10^{-4} - 10^{-3}$) in our Solar system (e.g. Earth's ocean) compared to the elemental abundance ($D/H = 1.5 \times 10^{-5}$) indicates that at least a fraction of water in our Solar system originates from cold regions such as molecular clouds or outer protoplanetary disks. Laboratory experiments and quantum chemical studies play fundamental roles to understand the formation of COMs and isotope fractionation, and thus the chemical link between ISM and planetary matter.

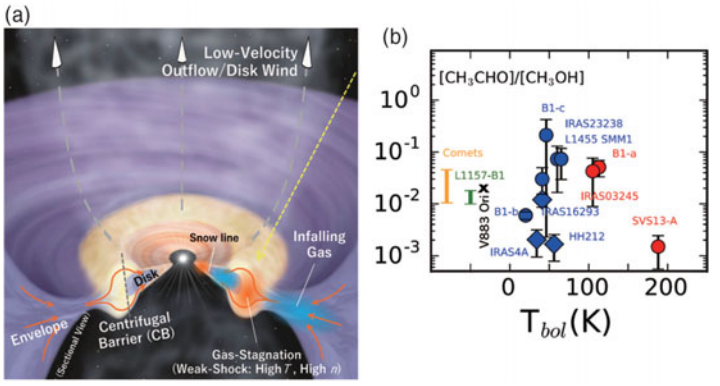

Figure 1. (a) Schematic view of a protostellar core from Sakai *et al.* (2017). (b) CH_3CHO/CH_3OH abundance ratios in hot corinos, comets, the protostellar shock L1157-B1, and in the disk around FU Ori star V883 Ori. Modified from Bianchi *et al.* (2019)

2. COMs in low-mass protostellar cores

2.1. *Observations of COMs around young stellar objects*

COMs are detected in the central ($r \leqslant 100$ au) region of several protostellar cores. The cores harboring COMs are called hot corinos. The excitation temperature of the lines typically ranges from several tens to a few hundreds K, indicating that the COMs are indeed in the central warm region of the core. IRAS16293 is a prototypical hot corino, towards which a molecular line survey has been performed with ALMA (Jørgensen *et al.* 2016). It is not straightforward to evaluate their column densities and relative abundances to hydrogen, due to the temperature and density gradient along the line of sight. Instead, COM abundances relative to CH_3OH are derived. CH_3OH is the most abundant COM observed so far, and is considered to be an important precursor of other COMs (e.g Öberg *et al.* 2009a). A typical sublimation temperature of COMs, including CH_3OH, is ~ 100 K. Typical abundances of COMs relative to CH_3OH are $10^{-3} - 10^{-2}$, which coincide with those in comets (e.g. Bianchi *et al.* 2019) (Figure 1b).

In the central region of the protostellar cores, protoplanetary disks with Keplerian rotation are being formed. Disks with a radius of ~ 100 au are found around several young protostars (Class 0-I), while the disk size is much smaller in some other objects (Yen *et al.* 2017). The disk is fed by the infall of the envelope, which is a dense gas around the protostar. Since each region is characterized by specific velocity field (infall vs Kepler rotation), we can distinguish the molecular composition in the envelope and the disk with the help of Doppler shifts. Sakai *et al.* (2014) found there is a transition zone, called centrifugal barrier, between the infalling envelope and Keplerian disk; it could be heated by weak accretion shock onto the forming disk. Oya *et al.* (2016) found that the emission lines of COMs trace the transition zone around a protostar IRAS 16293 a. It indicates that COMs in hot corinos will indeed be incorporated to protoplanetary disks.

Another recent breakthrough is the detection of freshly sublimated COMs in the protoplanetary disk of V883 Ori (Lee *et al.* 2019). The object is known to be in outburst; the mass accretion from the disk to the central star is temporally increased. The enhanced stellar luminosity ($\sim 400 L_\odot$) and the release of gravitational energy heat the disk. The water snow line, the radius at which the disk midplane temperature reaches the sublimation temperature of water (~ 100 K), is expected to be shifted to the radius of ~ 40 au, while it is usually located at a few au from the central star and thus difficult to observe in normal quiescent disks. Various COMs such as CH_3OH, CH_3CHO, CH_3OCHO, and

https://doi.org/10.1017/S1743921319008263 Published online by Cambridge University Press

CH_3COCH_3 are detected around the water snow line in the disk of V883 Ori. Since the duration of outburst (~ 100 yr) is shorter than the typical timescale of gas-phase reactions, the observed COM abundances reflect the chemical composition of ices in the disk before the outburst. Their abundances are similar to those in comets except for CH_3CN, which is less abundant in V883 Ori.

2.2. *COM formation mechanisms*

While ALMA has been playing an essential role in the investigation of organic chemistry in star forming regions, we should note that it tends to be biased to the gaseous species in warm compact regions. Laboratory experiments and theoretical models suggest that COMs form more efficiently in the ice mantle rather than via gas-phase reactions (e.g. Herbst & van Dishoeck 2009; Linnartz *et al.* 2015). The observation of organic molecules in solid (ice) phase is possible via infrared absorption bands, but the identification of molecular species is not as straightforward as the gas-phase observations at radio wavelengths (see review by Boogert in this volume). COM emission lines have been also detected in cold dense cores by single dish observations (Taquet *et al.* 2017 and references therein). It indicates that the formation of COMs starts in the cold ISM. A combination of quantitative understanding of chemical processes and star formation processes is needed to fully understand the evolution of organic molecules from the ISM to planetary matter (e.g. Aikawa 2013).

Laboratory experiments and theoretical models have indicated that COMs formation indeed starts in cold molecular clouds. In dense ($\geqslant 10^5$ cm^{-3}) cold (~ 10 K) cloud cores, even molecules as volatile as CO freeze-out onto grains. In the ice mantle, hydrogenation of CO forms HCO, H_2CO, and eventually CH_3OH, while H atom also abstracts hydrogen from stable molecules (e.g. CH_3OH) to form radicals (e.g. Hidaka *et al.* 2009). If the abundances of radicals such as HCO become high enough, they can react with each other to form more complex organics such as $HC(O)OCH_3$ (Chuang *et al.* 2016, see also Chuang *et al.* in this volume). Reactions can also be activated by cosmic-ray particles, which trigger radiation chemistry (Shingledecker *et al.* 2018, see also Shingledecker in this volume). The dust temperature starts to rise in the central region of the core, when the heating by the gravitational collapse overwhelms the radiation cooling. Then thermal diffusion of radicals enhances the formation of COMs, while the hydrogenation becomes inefficient due to the desorption of H atoms. A fraction of molecules and radicals desorb thermally or non-thermally (e.g. chemisorption) (e.g. Chuang *et al.* 2018), and could freeze-out again when they are converted to less volatile molecules via gas-phase reactions. Eventually, the gas and dust particles accrete to the central region of the core with $T \geqslant 100$ K. Most of COMs would be sublimated together with water, which is the dominant component of bulk ice mantle (Herbst & van Dishoeck 2009 and references therein).

While the above scenarios of COM formation, especially the importance of ice-phase chemistry, is currently the consensus within the community, there have been active investigations and discussions on the rate-limiting processes such as diffusion of radicals, and mathematical formulation of the reaction systems (Figure 2). In cold cores, for example, the diffusion of radicals in the ice mantle would be so limited, that they would react only with species in the neighboring adsorption sites. The ice chemistry then depends on local concentration of radicals. Microscopic Monte Carlo simulation, which records the position of each adsorbed species in ice mantle, is suitable for such cold ice chemistry (e.g. Cuppen *et al.* 2018) (see also Garrod & Clements on page 429). Microscopic Monte Carlo simulation is, however, computationally expensive; most of the CPU time is consumed to follow the thermal hopping of very volatile species such as H atom, once the temperature starts to rise.

https://doi.org/10.1017/S1743921319008263 Published online by Cambridge University Press

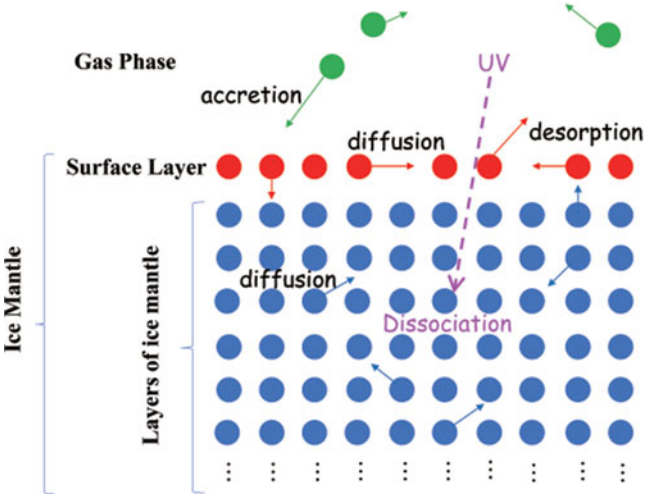

Figure 2. Schematic view of gas-grain chemistry.

The rate equation model, on the other hand, calculates the mean abundances of species in the ice mantle (and also in the gas phase). Most rate equation models assume Langmuir-Hinshelwood mechanism; i.e. the rate coefficient is proportional to the diffusion rate and mean concentration of reactants. The barrier of diffusion is thus the important parameter, which is often assumed to be $30-80$ percent of the desorption barrier of each species. The classical rate equation models that consist of the gas phase and the ice phase species are called two-phase models; these assume a constant barrier for diffusion (and desorption) of an icy species, while in reality species in the ice surface can desorb and thermally migrate more efficiently than those in bulk ice mantle. Hasegawa & Herbst (1993) constructed rate equation models which discriminate ice surface layers from bulk ice mantle (i.e. three-phase model). In recent years, the importance of such layering structures are re-recognized; several groups are currently using the three-phase model, and/or the rate equation models with the multi-layered structure of ice mantles (e.g. Fayolle *et al.* 2011; Taquet *et al.* 2012; Garrod 2013; Ruaud *et al.* 2016; Furuya *et al.* 2017).

Consideration of layered ice mantle and photodissociation of icy molecules are crucial for the formation of COMs. Lu *et al.* (2018) recently constructed a Macroscopic Monte Carlo model, which consists of ice surface layer and semi-active bulk ice mantle (and the gas phase) and investigated the chemical evolution from cold prestellar cores to hot corinos. They showed that the abundant radical species can be formed by photolysis and stored in bulk ice mantle in the cold core stage, and that these radicals form COMs upon warming up due to star formation. The COM abundances produced in the model are orders of magnitude higher than those in the two-phase model or the three-phase model with inert bulk ice mantle, and agree better with observations of hot corinos.

The diffusion rate of radicals and molecules are investigated intensively in laboratory experiments, molecular dynamics simulations, and quantum chemical calculations (e.g. Cuppen *et al.*, Theule *et al.*, Watanabe *et al.*, Sameera *et al.* and Miyazaki *et al.* in this volume). In water-dominated ice, for example, Ghesquiere (2015) showed that diffusion of small molecules such as CO_2 is determined by the self-diffusion of water molecules. Alternatively, diffusion in bulk ice mantle could be dominated by surface diffusion in cracks and pores. Then the structural evolution of ice mantle such as crack opening could affect the ice mantle chemistry (Ghesquiere 2018). A comparison of radiation chemistry

https://doi.org/10.1017/S1743921319008263 Published online by Cambridge University Press

model with laboratory experiments, on the other hand, indicates that radicals react with neighboring species rather than diffuse within ice mantle (Shingledecker *et al.* 2019).

2.3. *Variation among cores*

While the hot corinos are intensively observed, it is note worthy that not all protostellar cores are hot corinos. L1527, for example, is characterized by emission of unsaturated carbon chains, and emission lines of CH_3OH and other COMs are weak or not detected. Since unsaturated carbon chains are considered to form via gas-phase reactions of sublimated CH_4, the variation of chemical composition among protostellar cores could be due to the initial ice abundance ratio of CH_4 and CH_3OH, which in turn reflects the physical condition of parent molecular clouds. For example, if the visual extinction of parent clouds are relatively low, the formation of CO (via hydrocarbon) is delayed, which could results in a low ice abundance ratio of CH_3OH/CH_4 and then low (high) COM (carbon chain) abundances in the protostellar phase (e.g. Sakai & Yamamoto 2013).

Aikawa *et al.* (in prep) investigated the chemical evolution from molecular clouds to protostellar cores varying the physical parameters of parental clouds using the gas-grain chemical model with multi-layered ice mantle. The models show that there are multiple pathways to form CH_3OH and COMs. For example, in a model with relatively low initial visual extinction, CH_3OH can be formed via $CH_3 + OH$, instead of the hydrogenation of CO, in the ice mantle. Thanks to the multiple formation pathways, the COM abundances as a whole are not very sensitive to the initial cloud conditions. Formation of CH_3OH from hydrocarbons has been recently investigated in laboratory experiments, as well (Qasim *et al.* 2018; Bergner *et al.* 2019). The absence of COM emission then could be due to the current temperature structure of the protostellar cores. Since COMs are sublimated at $\geqslant 100$ K, the emission would be diluted if the sublimation region is much smaller than the beam size of the observation. It should also be noted that COMs are destroyed by gas-phase reactions after sublimation. The spatial distribution of gas-phase COMs is determined by the competition between the destruction and dynamics of the flow. If they are sublimated inside the Keplerian disk, the gas-phase destruction timescale is shorter than the radial accretion timescale; gaseous COMs would be abundant only in a narrow ring region around their snow line and thus hard to detect.

3. Isotope fractionation

3.1. *Fractionation mechanisms*

There are two well-known mechanisms of isotope fractionation: exothermic exchange reactions and isotope selective photodissociation. A good example of the former is Deuterium enrichment; the heavy isotopologue of a molecule has a lower zero-point energy than its normal isotopologue. The mass difference and thus the exothermicity of exchange reactions is especially large for D/H. While there are several exchange reactions, the reaction of

$$H_3^+ + HD \rightarrow H_2D^+ + H_2 \tag{3.1}$$

has the exothermicity of $\leqslant 230$ K, depending on the combinations of the spin states (ortho/para) of reactants and products, and plays the dominant role at low temperature (~ 10 K) (Hugo *et al.* 2009). Carbon is also known to fractionate via

$$CO + {}^{13}C^+ \rightarrow {}^{13}CO + C^+. \tag{3.2}$$

In molecular clouds, where CO is the dominant carbon reservoir, the $^{12}CO/^{13}CO$ ratio cannot significantly deviate from the elemental abundance ratio of $^{12}C/^{13}C = 60$, while the reaction tends to deplete ^{13}C from other molecules (Furuya *et al.* 2011).

https://doi.org/10.1017/S1743921319008263 Published online by Cambridge University Press

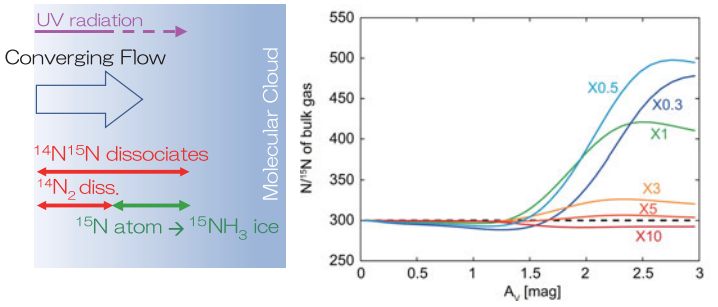

Figure 3. (a) Nitrogen fractionation during the molecular cloud formation. (b) The $^{14}N/^{15}N$ ratio of bulk gas phase as a function of visual extinction in the forming molecular cloud from Furuya & Aikawa (2018).

The latter mechanism, the selective photodissociation, is considered to be responsible for the oxygen isotope fractionation. When the gas of interstellar clouds or protoplanetary disks is irradiated by UV radiation, molecules are photodissociated. The photodissociation rates decrease with depth into the gas, as UV radiation is attenuated by dust (Figure 3a). But some specific molecules, such as CO are self-shielded at shallow depth; since they are relatively abundant and mainly dissociated by line absorption rather than continuum UV radiation, the dissociating photons are efficiently shielded by the line absorption. Then their rare isotopologues are selectively photodissociated at an intermediate depth, e.g. $A_v \sim 1$ mag, where the line shielding is effective for the major isotopologue, but not for rare ones. Selective photodissociation of $C^{18}O$ and $C^{17}O$ enhances the abundances of atomic ^{18}O and ^{17}O, which then could be converted to the heavy isotopologues of water. It is considered to be the heavy end member of the oxygen isotope fractionation diagram of planetary material in the Solar system; oxygen isotope ratios of meteorites, Earth, and Mars are on the mixing line between the heavy water and the Solar abundance (McKeegan 2011 and references therein).

3.2. *Nitrogen isotope fractionation*

Fractionation of nitrogen isotopes has long been debated. Primordial Solar system material such as comets and meteorites are enriched with ^{15}N by a factor of up to several compared to the Solar value ($^{14}N/^{15}N$=440) (Marty *et al.* 2011; Mumma & Charnley (2011)). The exchange reactions have been expected to be responsible for the enrichment of ^{15}N. Roueff *et al.* (2015), however, found that several major exchange reactions actually have activation barriers and thus do not proceed at low temperature (see also Wirstrom & Charnley (2018)).

Nitrogen isotope fractionation is also observed in low-mass dense cores. It should be noted that the current elemental abundance of $^{14}N/^{15}N$ in our Solar neighborhood is different from the Solar abundance due to the nucleonsynthesis in past 4.5 G years . The ratio is estimated to be $200-300$ based on the absorption line observations (e.g. CN) towards diffuse clouds (Ritchey *et al.* 2015). Compared with this elemental abundance, the N_2H^+ is strikingly enriched in ^{14}N; $N_2H^+/^{15}NNH^+$ is 1110 $\pm$240 in a prototypical prestellar core L1544 and >600 in B1 (Bizzocchi *et al.* 2013; Daniel *et al.* 2013). Recently, Furuya *et al.* (2018) found that $^{14}N/^{15}N$ ratio of N_2D^+ is also high $\geqslant 700$ in L1544, which suggests that the degree of fractionation does not significantly change with the depth to core center. The ^{14}N enrichment in N_2H^+, and its parental molecule N_2, cannot be explained by the exchange reactions, since the exchange reactions enrich molecules with

https://doi.org/10.1017/S1743921319008263 Published online by Cambridge University Press

heavy isotopes. In-situ selective photodissociation is effective only at $A_v \leqslant$ a few mag, and thus cannot explain the fractionation throughout the core.

Furuya & Aikawa (2018) found the ^{15}N enrichment in cometary ice and ^{14}N enrichment in the gas of prestellar core can be explained by selective photodissociation in the formation stage of molecular clouds (Figure 3a). Our Galaxy is filled with expanding shell-like structures due to gas flows from mass loss stars. Molecular clouds are formed by the conversing flow when two or more expanding shells meet; cold and dense gas is formed behind the shock (e.g. Inoue & Inutsuka 2012). Furuya & Aikawa (2018) calculated gas-dust chemical reaction network with isotope fractionation behind the shock front in 1D steady shock model. The rate equation method with layered ice mantle is adopted. At $A_v \sim 1-2$ mag, the selective photodissociation of $N^{15}N$ enhances the abundance of gaseous ^{15}N atoms, which are then adsorbed on to grains to be converted to NH_3 ice. While the selective photodissociation is effective only at a limited range of A_v, all gas passes through this region to be incorporated to the molecular clouds. Then bulk gas in molecular clouds becomes ^{14}N rich, while the ice phase becomes ^{15}N rich. The fractionation between the gas and ice phases remains until NH_3 ice sublimates around protostars or inside the snow line in protoplanetary disks.

In the model of Furuya & Aikawa (2018), NH_3 ice is mainly destroyed by photodesorption. While the photodissociation of NH_3 ice is also included in the model, a significant fraction of photo-fragments are hydrogenated to reform NH_3 ice. Then the photodesorption yield determines the efficiency of NH_3 freeze-out, which is essential for the fractionation of nitrogen isotope between gas and ice. In their fiducial model, the yield of 1×10^{-3} is adopted referring to the laboratory experiment of water ice and NH_3 ice (Öberg *et al.* 2009b; Martin-Domenech *et al.* 2018). Figure 3(b) shows that the $^{14}N/^{15}N$ ratio in the bulk gas sensitively depends on the photodesorption yield.

References

Aikawa, Y. 2013, *Chem. Rev.*, 113, 8961
Bergner, J., Öberg, K. I., Rajappan, M., *et al.* 2019, *ApJ*, 874, 115
Bianchi E., Codella, C., Ceccarelli, C., *et al.* 2019, *MNRAS*, 483, 1850
Bizzocchi, L., Caselli, P., Leonardo, E., *et al.* 2013, *A&A*, 555, 109
Chuang, K.-J., Fedoseev, G., Ioppolo, S., *et al.* 2016, *MNRAS*, 455, 1702
Chuang, K.-J., Fedoseev, G., Qasim, D., *et al.* 2018, *ApJ*, 853, 102
Cuppen, H., Fredon, A., Lamberts, T., *et al.* 2018, *IAU Symposium*, 332, 293
Daniel, F., Gélan, M., Roueff, E., *et al.* 2013, *A&A*, 560, 3
Fayolle, E. C., Öberg, K. I., Cuppen, H., *et al.* 2011, *A&A*, 529, 74
Furuya, K., Aikawa, Y., Sakai, N., *et al.* 2011, *ApJ*, 731, 38
Furuya, K., Drozdovskaya, M. N., Visser, R., *et al.* 2017, *A&A*, 599, 40
Furuya, K. & Aikawa, Y. 2018, *ApJ*, 857, 105
Furuya, K., Watanabe, Y., Sakai, T., *et al.* 2018, *A&A*, 615, 16
Garrod, R. T. 2013, *ApJ*, 765, 60
Ghesquiere, P., Mineva, T., Talbi, D., *et al.* 2015, *PCCP*, 17, 11455
Ghesquiere, P., Ivlev, A., Noble, A., *et al.* 2018, *A&A*, 614, 107
Hasegawa, T. I. & Herbst, E. 1993, *MNRAS*, 263, 589
Herbst, E. & van Dishoeck, E. F. 2009, *ARA&A*, 47, 427
Hidaka, H., Watanabe, M. Kouchi, A., *et al.* 2009, *ApJ*, 702, 291
Hugo, E., Asvany, O., Schlemmer. S., 2009, *J. Chem. Phys*, 130, 164302
Inoue, T. & Inutsuka, S. 2012, *ApJ*, 759, 35
Jørgensen J. K., van der Wiel, M. H. D., Coutens, A. *et al.* 2016, *A&A*, 595, 117
Martin-Domenech, R., Cruz-Diaz, G. A, Muñoz Caro, G. M., *et al.* 2018, *MNRAS*, 473, 2575
Marty, B., Chaussidon, M., Wiens, R. C., *et al.* 2011, *Science*, 332, 1533
McKeegan, K. D., Kallio, A. P., Heber, V. S., *et al.* 2011, *Science*, 332, 1528

https://doi.org/10.1017/S1743921319008263 Published online by Cambridge University Press

Mumma & Charnley 2011, *ARA&A*, 49, 471
Lee, J.-E., Lee, S., Baek, G. *et al.* 2019, *Nature Astron.*, 3, 314
Linnartz, H., Ioppolo, S., Fedoseev, G. 2015, *Int. Rev. Phys. Chem.* 34, 205
Lu, Y., Chang, Q., Aikawa, Y., *et al.* 2018, *ApJ*, 869, 165
Öberg, K. I., Garrod, R. T., van Dishoeck, E. F., & Linnartz, H. 2009, *A&A*, 504, 891
Öberg, K. I., Linnartz, H., Visser, R., *et al.* 2009, *ApJ*, 693, 1209
Oya, Y., Sakai, N., López-Sepulcre, A., *et al.* 2016, *ApJ*, 824, 88
Qasim, D., Chuang, K.-J., Fedoseev, G., *et al.* 2018, *A&A*, 612, A83
Ritchey, A. M., Federman, S. R., Lambert, D. L., *et al.* 2015, *ApJL*, 804, L3
Roueff, E., Loison, J. C. Hickson, K. M., *et al.* 2015, *A&A*, 576, 99
Ruaud, M., Wakelam, V., Hersant, F., *et al.* 2016, *MNRAS*, 459, 3756
Sakai, N. & Yamamoto, S. 2013, *Chem. Rev.*, 113, 8981
Sakai, N., Sakai, T., Hirota, T., *et al.* 2014, *Nature*, 507, 78
Sakai, N., Oya, Y., Higuchi, A., *et al.* 2017, *MNRAS*, 467, 76
Shingledecker, C. N., Tennis, J., Le Gal, R., *et al.* 2018, *ApJ*, 861, 20
Shingledecker, C. N., Vasyunin, A., Herbst, E., *et al.* 2019, *ApJ*, 876, 140
Taquet, V., Ceccarelli, C., Kahane, C., *et al.* 2012, *A&A*, 538, A42
Taquet, V., Wirstr'om, E. S., Charnley, S. B., *et al.* 2017, *A&A*, 607, A20
Wirstrom & Charnley 2018, *MNRAS*, 474, 3720
Yen H.-W., Koch, P., Takakuwa, S., *et al.* 2017, *ApJ*, 834, 178

https://doi.org/10.1017/S1743921319008263 Published online by Cambridge University Press